Two climate-sensitive tree-ring chronologies from Arnhem Land, monsoonal Australia

Allen, K.J.[1,2*], Brookhouse, M.[3], French, B.J.[4], Nichols, S.C.[1], Dahl, B.[3], Norrie, D.[3], Prior, L.D.[4], Palmer, J.G.[2,5], Bowman, D.J.M.S.[4]

[1] School of Ecosystem and Forest Science, University of Melbourne, 500 Yarra Boulevard, Richmond, Victoria, Australia 3121

[2]ARC Centre of Excellence in Australian Biodiversity and Heritage, University of New South Wales, Sydney, NSW 2052, Australia.

[3]School of Biology, Australian National University, 134 Linnaeus Way, Acton ACT, Australia 2601

[4] School of Natural Sciences, University of Tasmania, College Rd, Sandy Bay, TAS Australia 7005

[5] School of Biological, Earth and Environmental Sciences, University of New South Wales, Sydney, NSW 2052, Australia.

[*] Corresponding author

Acknowledgements

We wish to acknowledge the traditional custodians of the land from which the samples used in this study were collected – the Iwaidja and Gunwinggu/Guenei people – and wish to pay our respect to their elders; past, present and emerging. We also acknowledge Gilbert Tutty and Brian Delaney who assisted Graeme Hammer with the collection of the cores from Murganella (MUR). A CERF grant (B0016193) supported some of the collection of samples from the KOR site, and DP0878744 also provided some support for KA. We appreciate computing assistance from Mike Sumner and thank two anonymous reviewers whose constructive comments led to substantial improvements in this manuscript.

Abstract

The ecology of the Australian monsoon tropics is fundamentally shaped by dry conditions between May and October followed by highly variable rainfall over the months of November to April. Due to its crucial ecological importance, a better understanding of past hydroclimate variability in the region is of great interest. Temporally shallow and geographically patchy instrumental record also make highly resolved terrestrial palaeoclimate records for northern Australia prior to 1900 CE of considerable scientific importance. Here we present two new well-replicated *Callitris intratropica* ring-width chronologies from Arnhem Land in northern Australia, one of which extends the tree-ring record in the region by another 86 years, back to 1761. Both chronologies have clearly defined regional patterns of correlations with temperature, precipitation, potential evapotranspiration and two drought indices (the self-calibrating Palmer Drought Severity Index (PDSI) and the Standardised Precipitation Evapotranspiration Index (SPEI)) across the lower latitudes of the Northern Territory. Results indicate considerable scope for hydroclimatic reconstructions based on *C. intratropica* for transitional periods into and out of the wettest time of the year. This suggests such reconstructions would reflect variability in the duration of the wet period. While precipitation or streamflow reconstructions may be possible for both these transitional periods, drought reconstructions will be best focused on the months of March-May at the end of the wet period. Hydroclimate reconstructions would provide important baseline information for understanding the rate and magnitude of current regional climate change for these ecologically and culturally important transitional periods.

Key words: *Callitris intratropica*, northern Australia, dendrochronology, hydroclimate, SPEI, ecological processes, Indigenous weather calendars

Introduction

The Australian monsoon tropics is characterised by strongly contrasting seasons, from hot dry and flammable conditions between May and October, and wet conditions between November and April. The hydroecology of the region fundamentally shapes the ecology, distribution and abundance of most flora and fauna as well as indigenous land management practices (Woinarski et al., 2007). While northern Australia is most commonly associated with monsoonal rain, extra-monsoonal rainfall, associated with local convective storms, and its temporal pattern is crucial to these ecological processes (Cook and Heerdegen, 2001), affecting, for example, feeding habits, breeding, flowering and fruiting and species migration. With its very high floral and faunal endemism (Woinarski et al., 2006), the biodiversity of the northern part of the Northern Territory is both nationally and internationally significant (Woinarski et al., 2007). Variability in extra-monsoonal rainfall can have critical impacts on threatened species or species highly dependent on specific conditions (Woinarski et al., 2007) and changes in rainfall seasonality across a number of tropical regions have previously been noted (Feng et al., 2013).

A lack of long instrumental record for the region makes it difficult to assess the contribution of past hydroclimate to ecological change in the region. Increased interest in agricultural and regional development in parts of the Northern Territory in recent times (see CSIRO research summary: https://www.csiro.au/en/Research/Major-initiatives/Northern-Australia/Current-work/NAWRA) also raises the possibility of increased pressures on this highly seasonal environment. This lack of baseline information, potentially increasing land use pressures and general concerns about the impacts of climate change across Australia highlight a need for longer, well-replicated and absolutely dated records of past hydroclimate variability in northern Australia.

Dendrochronological records have the potential to provide high-resolution climate records. Historically, the majority of Australian dendroclimatic work has relied upon tree-ring chronologies from the continent's temperate south, with a particular focus on Tasmania in the mid-latitudes. This focus reflects the known reliable production of annual rings in the southern long-lived endemic conifer species (e.g. Cook et al, 2000; Buckley et al., 1997; Allen et al., 2001; 2011; 2017). Conversely, Australia's monsoonal north has received relatively little dendrochronological attention. As the temperate southern and monsoonal northern regions are subject to very different climate regimes, and the roles played by the various ocean-atmosphere processes differ between the two regions, the southern tree-ring chronologies cannot be expected to reflect climatic variability in the north (Allen et al., 2018).

Although significant efforts have led to a gradual increase in the number of dendrochronological studies for mainland Australia over the past couple of decades (e.g. Pearson and Searson, 2002; Baker et al., 2008; Heinrich et al., 2008; 2009; Cullen and Grierson, 2007; 2009; O'Donnell et al., 2010; 2015; 2018; Santini et al., 2013; Pearson et al., 2011;Witt et al., 2017; Haines et al., 2018a and b), only four geographically dispersed sites (D'Arrigo et al., 2008; Heinrich et al., 2008; Cullen and Grierson, 2009; O'Donnell et al., 2015; 2018; Palmer et al., 2015) have so far been used to generate annually resolved climate reconstructions. All of these are hydroclimate reconstructions, and three are based on *Callitris* spp.

The genus *Callitris* is a widespread, evergreen and taxonomically complex drought-tolerant group of species (Piggins and Bruhl, 2010; Sakaguchi et al., 2013) in the family Cupressaceae. There are around 13 species endemic to Australia (Farjon, 2010), and an additional species restricted to New Caledonia. Dendrochronological dating of *Callitris* has been hampered by the formation of frequent false rings, particularly in more arid environments (Pearson et al., 2011). Nevertheless, several

studies have demonstrated the potential to develop chronologies from the genus in seasonally dry regions of the continent's north and west (Ogden, 1981; Baker et al., 2008; Cullen and Grierson, 2009; O'Donnell et al., 2010; Pearson et al. 2011). One of the species in this genus, *Callitris intratropica*, distributed across much of monsoonal Australia, is extremely drought tolerant (Brodribb et al., 2010; 2013), resilient to termite attack but sensitive to intense fire (Yates and Russell-Smith 2003; Russell-Smith 2006; Bowman et al., 2014; 2018). The size class distribution of living and dead stems has been the basis for a number of landscape ecology studies (e.g. Bowman and Panton, 1993; Prior et al., 2004a; 2010; 2011; Trauernicht, 2012) and the species has commonly been considered an indicator of general ecosystem health, although this has recently been called into question (Radford et al., 2013). Individuals of the species growing in monospecific stands generally reach maturity later than isolated individuals that also have a faster growth rate (Lunt et al., 2011; Lawes et al., 2013). The first details of successfully cross-dated *C. intratropica* chronologies in Australia's far north emerged in 2008, with Baker et al. (2008) reporting annual rings in *C. intratropica* chronologies and the ability to identify false rings in young trees of known age. The same study then produced a successfully crossdated chronology from older non-plantation trees. A continental-scale study subsequently verified, by means of accelerator mass spectrometry to measure ^{14}C content of samples, the annularity of tree-ring formation in *C. intratropica* at some north Australian sites (Pearson et al., 2011).

Baker et al. (2008) also provided the initial detailed information concerning the response of ring widths *C. intratropica* to temperature, precipitation and the self-calibrating Palmer Drought Severity Index (sc-PDSI; Wells et al., 2004), thereby laying the first solid foundations for high quality reconstructions from the species. This information provided the essential context for the inclusion of the species in two later broadscale drought reconstructions (September-January; D'Arrigo et al 2008 and

December-February; Palmer et al. 2015) based on the sc-PDSI. Further detailed physiological work has noted that although *C. intratropica* is highly drought tolerant (Brodribb et al., 2010; 2013), water availability clearly plays a critical role in the addition of annual increment in this species (Baker et al., 2008; Brodribb et al., 2010; 2013; Drew et al., 2011; 2014). Growth typically begins soon after rain begins to reliably fall in November, ceasing in April/May (Prior et al., 2004b; Drew et al., 2014).

Although there is increasing impetus to develop long climate reconstructions using this species, there are two immediate challenges to this goal in monsoonal Australia. Firstly, there are very few published chronologies for this region (three), and those that have been published are either short and/or have low sample depths ($n \leq 10$) over much of their length. Higher replication is likely to improve the quality of the climate signal present in the ring widths. Secondly, the variability in tree growth responses to climate variability across the broader region (e.g. Baker et al., 2008; Cullen and Grierson, 2009; O'Donnell et al., 2018) and the different climate regimes at existing and potential sites across northern Australia, highlights a need to better understand the spatial extent over which climate signals are preserved by *C. intratropica*. The relationships shown by Baker et al (2008) were based on single-point climate data and therefore did not explore the geographical extent of the climate signal contained in the ring widths of a single site. Such spatial information is relevant for climate field reconstruction.

In this study, our primary objective is to present and describe two well-replicated *C. intratropica* chronologies from Arnhem Land, northern Australia. An important part of this description is an assessment of whether there are coherent regional responses to climate variables such as temperature, precipitation, evapotranspiration and drought across the Australian region from 11-15.25°S and 130-136.5°E. This provides crucial background to assessing the suitability of the sites for

155 future climate field reconstructions of these variables. We also compare the regional
156 responses of our two new sites with those outlined by Baker et al. (2008) for single
157 point data. Specifically, we aim to address the question of whether these two sites will
158 be useful in hydroclimatic reconstructions for this region, and, if so, for what months
159 and what hydroclimatic variables.

160 **Materials and Methods**

161 *Geographic setting*

162 The two new *C. intratropica* sites, Korlobirrahda (KOR) and Murganella
163 (MUR) are located approximately 220 km apart in Arnhem Land (Figure 1) in a
164 landscape with relatively little topographical variability that experiences a strongly
165 seasonal climate. The KOR site builds upon and extends the original KOR chronology
166 shown by Pearson et al (2011).

167 On average, 94% of precipitation falls between November and April (Figure 2a)
168 and average annual rainfall ranges from 1000-1500 mm across the far north of the
169 region, increasing to 2000-3000 mm annually around Darwin. There are typically 50 -
170 75 days with more than 5mm of rainfall (www.bom.gov.au) in the far north, this rapidly
171 decreases as latitude increases. Based on a 20-year period, Cook and Heerdegen (2001)
172 estimated this decrease to be in the order of ~50% over 8 degrees of latitude. Overall,
173 precipitation over the region has increased since the start of records (Figure 2c&d;
174 Mann-Kendall test for trend: Darwin, $p = 0.0128$; Katherine, $p = 0.0807$; Oenpelli, $p =$
175 0.003; Warruwi, $p = 0.619$), although the strength of the trend depends upon the period
176 examined (Woinarski et al., 2007; www.bom.gov.au). Increased rainfall appears mainly
177 related to increased intensity of events (Smith et al. 2006).

178 Maximum temperatures across the study region are highest from October - April
179 (34-37°C on average; Figure 2a) compared to a low of 29-30°C in June-July. Minimum

temperatures range from ~14°C in July to ~24°C from November-February. There are some subtle differences between the two tree-ring sites with average June – September minimum temperatures at the inland site, KOR, being slighter lower than at the more coastal site, MUR. Evapotranspiration is generally higher at MUR all year round (www.bom.gov.au). Temperatures at Darwin, the closest station in the Bureau of Meteorology's ACORN-SAT network that provides homogenised temperature records from ground-based stations, illustrate that the increase in both maximum and minimum temperatures since the start of the record in 1910 (Figure 2b) is highly significant (Mann-Kendall test for trend; p = 2.22e-16).

Sampling and chronology development

Samples from KOR were collected over successive field trips between 2006 and 2016 by Bowman and co-workers as part of a broad scale ecological study (Prior et al., 2011). Sampled trees grew either in small groves or as single trees in open savannah areas. Samples from the region around Murganella were collected from small monospecific stands in the early 1970s for species-level growth modeling (Hammer, 1981; 1983). Maps marked with locations of groves at MUR indicate they are scattered across the landscape around Murganella, and this may become relevant when considering the climate-tree-ring width relationship at MUR. Importantly, samples from neither site were collected with dendroclimatological work in mind, but the sheer number of samples for both sites and the temporal depth, makes them of particular interest for climate studies.

All samples were prepared in accordance with standard dendrochronological techniques (Stokes and Smiley 1968). Coorecorder in combination with CDendro image analysis software (http://www.cybis.se/forfun/dendro/) was used to measure ring widths and the crossdating data quality control COFECHA software (Holmes 1983)

used to check visual crossdating (temporal matching of ring widths across samples). In order to examine climate influences on incremental tree growth, it is necessary to first remove nonclimatic variability (Fritts, 1976). Trees at both KOR and MUR typically exhibit declining growth-ring width with age, as commonly observed in many species in relatively open habitats (cf. Fritts 1976). Therefore, a negative exponential/linear regression line detrending regime was used to detrend tree ring-width series at both sites. Site-level skeleton plots that identify particularly narrow rings compared to their neighbours were produced using the dplR package in R (Appendix S1; Bunn 2010). We produced our chronologies in the signal-free environment (Melvin and Briffa, 2007) to avoid or reduce distortion of final chronologies due to the removal of decadal-centennial frequency information common across the site that may well be associated with climate. This variability may be removed with standardisation techniques that fit a growth curve (in this case a negative exponential curve/linear regression line) to the data directly. Signal-free standardisation is an iterative procedure that first removes a common site signal from the data prior to fitting a growth curve to an individual tree-ring series (see Melvin and Briffa 2008 for details).

Climate data and Analyses

To assess the strength of relationships between each of the two chronologies and the climate parameters, we examined Pearson correlations for autoregressively modeled data. This was done over the full period of overlap between each chronology (1902 – 2015 KOR; 1902 – 1973 MUR) and each point contained within the gridded data sets described below for the area bounded by latitudes 11 – 15.25°S and longitudes 130 – 137.5°E. This area encapsulates the far north of the Northern Territory (Figure 1) and is approximately 291,000km^2.

The temperature data, potential evapotranspiration and SPEI and scPDSI extended from 1902 – 2015 and precipitation data covers the period 1901-2016. All gridded data sets used have a resolution of 0.5 x 0.5°. Climate variables included monthly and seasonal (December-February (DJF), March-May (MAM), June-August (JJA), September-November (SON)) mean, maximum and minimum temperature (107 grid cells), total precipitation (118 grid cells), potential evapotranspiration (107 grid cells) and two drought indices (each with 107 grid cells): the sc-PDSI and the Standardised Precipitation Evapotranspiration Index (SPEI; Vicente-Serrano et al., 2010a&b). The Climate Research Unit (CRU) temperature and potential evapotranspiration were downloaded from http://doi.org/10/gcmdf7; Harris et al., 2014), while precipitation data were sourced from the Global Precipitation Climatology Centre (GPCC; https://www.esrl.noaa.gov/psd/data/gridded/data.gpcc.html; Schneider et al., 2011; Becker et al., 2013). Because there is evidence that the number of rainfall events is relevant to growth in this species (Drew et al., 2014), we also compared the chronologies against the number of rain days per year/season at the two closest long-term high quality stations (Oenpelli 1910-2013 and Warruwi 1916-2017). Number of rain days is not available from the gridded monthly data, hence our reliance on these two stations. We used total rainfall and an imposed threshold of ≥ 5mm/day in accordance with Cook and Heerdegen (2001) who defined a rain day as one with > 5mm of rain because evapotranspiration typically exceeds this amount.

The two drought indices used in this study incorporate both precipitation and temperature in their calculation. As temperature is an important driver of evapotranspiration, drought indices incorporating it are more appropriate when considering plant drought sensitivity than indices depending only on precipitation. This point is well illustrated by, amongst others, Jeong et al. (2014). Cook et al. (2016) have

254 also demonstrated the crucial role of temperature in drought projections for eastern
255 Australia.

256 The sc-PDSI is a modification of the original PDSI (Palmer 1965) and calibrates
257 behavior of the index at a given location (Wells et al., 2004). It is based on a simple
258 bucket model of soil moisture and essentially measures the excess or lack of moisture
259 at a given point based on certain underlying assumptions and conditions as detailed by
260 Wells et al. (2004). The sc-PDSI is the basis of the tree-ring based drought atlases
261 including the North American Drought Atlas (NADA; Cook et al., 2007), the Monsoon
262 Asia Atlas (MADA; Cook et al., 2010), the Old World Drought Atlas (OWDA; Cook
263 et al., 2015), the Mexican Drought Atlas (MxDA; Stahle et al., 2016) and the Australia
264 New Zealand Drought Atlas (ANZDA; Palmer et al., 2015). The West Australian
265 Drought Atlas (WADA) will also be based on the sc-PDSI (O'Donnell et al., 2018).

266 While this legacy means that the potential to reconstruct the sc-PDSI using
267 *Callitris* from the Arnhem Land region is of considerable interest, limitations of this
268 index include its fixed temporal scale (monthly) and strong autocorrelative structure
269 (Guttman, 1998; Vicente-Serrano et al., 2010a). Drought, on the other hand may occur
270 over time-scales of months to years, and even short-term droughts may negatively affect
271 both plant growth and human societies. In contrast to the sc-PDSI, the SPEI represents
272 an accumulated moisture deficit calculated at different time scales (Vicente-Serrano et
273 al., 2010a&b). Once again, the index is based on moisture deficit, essentially the
274 difference between precipitation and potential evapotranspiration. The calculation
275 process used to scale the index is very similar to that used for the Standardised
276 Precipitation Index (SPI) index. Therefore, like the sc-PDSI it is based on water
277 balance in the soil, but can be calculated based on different time scales. This scaled
278 nature of the index allows the impact of droughts of different durations to be explored,
279 and a comparison with the sc-PDSI to be made. We examined the SPEI at times scales

of 1,3,6 and 12 months and the sc-PDSI averaged over the same periods. Data for the sc-PDSI and SPEI were obtained from the CRU data portal (https://crudata.uea.ac.uk/cru/data/drought/) and the repository of the Spanish National Research Council (CSIC: https://digital.csic.es/handle/10261/153475 respectively. Spatial correlations amongst the gridded data are shown and discussed in Appendix S2.

As a final hydroclimate comparison, we examined the relationship between the KOR chronology and streamflow at the Australian Bureau of Meteorology's (BOM) East Alligator hydrological reference station (12.72°S, 133.32°E, 460 mASL). There were two reasons to use this streamflow gauge. First, it is the closest station to the KOR site, and secondly, Verdon-Kidd et al. (2017) used this station as the basis for a long streamflow reconstruction that relied exclusively on remote proxies. We did not compare streamflow with MUR because this chronology ends in 1973 and the streamflow data does not commence until late 1971. We compared flows over the same windows identified above.

Results

The chronologies

The KOR chronology is comprised of 165 samples, and the MUR chronology of 69 samples (Table 1). Median segment length is 86 for KOR and 74 for MUR. Greatest sample depth for both chronologies occurs in the late 20th Century, only falling below five at 1774 CE (KOR), and 1848 CE (MUR) (Figures 3 and Appendix S1; Figure S2). There is no large discontinuity in sample start dates in the KOR chronology, although the first year of a large proportion of trees sampled in 2006 was between 1930 and 1960 (Appendix S1; Figure S2). First and last years in KOR are much more heterogenous than for MUR, reflecting the sampling of dead material at KOR, and the focus on live trees at MUR (Appendix S1; Figure S2). The start of the KOR chronology

is weak, but low sample depth at this point means it is not currently possible to assess where problems lie. For the purposes of this study, we have therefore retained all samples representing this time period in the chronology, but recommend that the earliest portion of it be cautiously used until additional samples can help resolve any dating issues.

The Expressed Population Signal (EPS; Wigley et al., 1984) for both chronologies is 0.8 or greater for much of their respective lengths, declining as sample depth declines (Figure 3). Overall, average EPS is greater than 0.9 for both chronologies (Table 1) and above the commonly cited 0.85 value at KOR from 1803 CE, and at MUR from 1846 CE. The average correlation amongst all possible pairs of samples (RBar) for KOR remains relatively stable between ~ 0.3 – 0.4, averaging 0.35 (Table 1). Average RBar for MUR is 0.42, exceeding 0.5 during the first two decades when replication is low but decreasing to 0.3 -0.4 as sample depth rapidly climbs from ~1880 CE onwards. The two chronologies share nine (1868, 1891, 1896, 1899, 1905, 1911, 1925, 1941 and 1945 CE) of 19 possible narrow rings (rings at least 1σ below the mean) identified after removing frequencies lower than 32 years as part of checking crossdating via COFECHA, and 14 of a possible 32 signature rings identified through a comparison of their skeleton plots (Appendix S1; Figure S1). Overall, the narrowest rings are 1951 CE at KOR and 1925 CE at MUR. Average lag 1 autocorrelation is relatively high at both sites (~0.57; Table 1).

With the exception of the start of MUR, inter-annual variability of the two chronologies is relatively consistent (Figure 3). Over the period for which both chronologies have sample depths greater than 10 (1859-1972), the correlation between the two chronologies is 0.55. That relationship breaks down at 1951, the narrowest ring in the KOR chronology (see Section S1 for a brief discussion of a missing ring in MUR). Although there appears to be some decadal variability in KOR, statistically

331 significant ($p < 0.05$) spectral peaks only occur at 64.1, 4.6 and 2.9 years. In the shorter
332 MUR series, statistically significant spectral peaks occur at 64.1 and 4.7 years (Figure
333 3). The limited length of both series means that the 64.1-year periodicity should be
334 treated with caution.

335 *Relationships with climate variables*

336 In this section, we focus on relationships with the data seasonalised across 3-
337 month periods previously identified (DJF, MAM, JJA, SON), while correlations with
338 monthly climate data are shown and discussed in Appendix S2. Monthly results for the
339 variously scaled SPEI- and scPDSI are also shown in Appendix S2. For a single site,
340 the slightly different periods of overlap with the climate data (different by two years for
341 precipitation compared to temperature) are unlikely to have any substantial impact on
342 the correlations shown.

343 There are consistent seasonal patterns in temperature-ring width relationships
344 across the region for the two sites (Figure 4). Strongest significant ($p < 0.05$)
345 correlations typically occur from March-May (Figure 4) when they are negative. The
346 strongest positive and significant ($p \leq 0.05$) grid-point correlations between both
347 chronologies and temperature occur in JJA. The largest difference across the three
348 temperature variables is the positive and significant ($p < 0.05$) correlations with SON
349 minimum temperature (Figure 4). Variability in the response to mean and maximum
350 temperature across the region is low for both sites, but slightly higher for MUR (see
351 also Appendix S2; Figure S3). Overall, there is greater variability in the response to
352 minimum temperatures.

353 For both sites, the variability in the response to precipitation is greater than that
354 to temperature (Figure 4). Overall, strongest positive relationships occur during SON
355 and MAM. The pattern is consistent with the single point precipitation data at Warruwi

and Oenpelli (Table 2; $0.18 \leq r \leq 0.43$; Figure S4 in Appendix S2) with marginally stronger relationships with both SON and MAM rainfall. Interestingly, the relationships with the number of rain days at these two rainfall stations, applying the 5mm threshold (0.16 - 0.63), were generally stronger than those with total rainfall amount (0 – 0.48; Table 2). Potential evapotranspiration in MAM is strongly and significantly ($p < 0.05$) negatively correlated with ring width at both sites (Figure 4). For MUR there are positive, but not always significant positive relationships in JJA.

The pattern of correlations with the gridded SPEI-3 is similar for the two chronologies (Figure 4) although there is greater spread in correlations for MUR (see also Appendix S2; Figure S5). In broad terms, relationships tend to be positive from July through to May, although there is something of an hiatus for DJF that is more obvious at KOR. Strongest correlations generally occur for April and May (KOR) and May (MUR).

Correlation between KOR and August-July streamflow at East Alligator river is negligible at r = -0.09, but the relationship becomes positive and marginally significant for SON (r = 0.276; $p < 0.1$; Figure 5) and MAM (r = 0.298; $p < 0.1$). A relatively strong but negative correlation with DJF streamflow (r=-0.31; $p < 0.1$; Figure 5), however, cautions against making firm conclusions regarding the strength of these relationships without additional data.

Discussion

Extending the chronology network in the far north

The central Arnhem Land chronology (KOR) extends back into the 18th Century, exceeding the length of any other north Australian *Callitris* chronologies thus far published by 86 years. Along with the Pine Creek (PC) chronology developed by

Baker et al. (2008), our two new chronologies make an important contribution to the development of a network of cross-dated chronologies for this part of the country.

Importantly, KOR is comprised of naturally occurring trees and includes long-dead trees, relatively young (~50 years) and old (> 100 years) trees, thus avoiding possible bias in climate relationships associated with tree age (e.g. Hanna et al., 2018). All previously published chronologies (PC; 1847-2006 and Howard Springs HS; 1965-2006) shown in Baker et al. (2008), and the early version of the KOR chronology (Pearson et al., 2011) rely exclusively on live trees. Additionally, all previously published chronologies of the species are considerably less well replicated in the early part of the 20th Century in particular (Baker et al. 2008; Pearson et al., 2011; Palmer et al., 2015), and include samples from far fewer trees (Table 1). The greater length of the new KOR chronology and the much improved replication of both MUR and KOR are the chief improvements offered by our chronologies for this region. Average EPS values for the longer Baker et al. (2008) and our new chronologies are almost the same although RBar is much higher in the PC chronology. This higher RBar is also reflected in a very high mean inter-series correlation (MISC) at PC (Table 1). Mean sensitivity of the three longer chronologies is again comparable while that for HS is relatively low (Table 1). The very high MISC and RBar for PC is likely associated with improvements made for climate reconstruction purposes (D'Arrigo et al., 2008). Originally, cores from 26 trees were collected, but only those from 14 trees have been included in the final chronology.

The Pearson et al. (2011) study identified additional collections of the species in the region (Figure 1), indicating considerable potential exists for additional sites.

Consistency with previous work

405 Although gridded data in regions with a low-density network of climate stations
406 such as this one must be treated with caution (Fu et al., 2015), the strength of our results
407 lies with the ability to identify general patterns across the region as well as their
408 consistency with the point comparisons made by Baker et al. (2008), particularly for
409 their PC chronology (Figure 4; Appendix S2). There is less consistency with the shorter
410 HS chronology, but Baker et al. (2008) found that patterns of correlations with climate
411 were not well defined for HS relative to PC. The relative youth of HS – deliberately
412 sourced from plantation trees of a known age (~40 years) to validate the annual nature
413 of rings in the species – is a likely reason for this difference. The general pattern of
414 response of our two sites to the monthly sc-PDSI and SPEI again indicates a regionally
415 consistent response (Appendix S2; Figures S5-S6) and is also consistent with results
416 for PC (Baker et al., 2008). Some differences between the two sites and potential
417 reasons for these are explored in the Supplementary material (Appendix S2, Figures
418 S8-9).

419 Our work also expands upon the results of Baker et al. (2008) by demonstrating
420 consistency in these climate relationships across the region (Figures 3, S3-5) and
421 showing that these relationships are more geographically coherent for temperature,
422 evapotranspiration and drought as defined by the SPEI and sc-PDSI than for
423 precipitation. Our investigation of multi-month windows also helps to further
424 consolidate foundations for future climate reconstructions.

425 It is also important that our statistical results accord with previous physiological
426 work on the species and ecological knowledge of the region. As described in the
427 Introduction, increment growth in the species is tied to the wet period of the year. In
428 relation to precipitation, Brodribb (2010; 2013) and Drew et al. (2011; 2014) have
429 found that larger growth increments are less related to total precipitation over the wet
430 season than to the frequency of rainfall events. Additional wet days over the SON and

MAM periods may be associated with wider growth rings; fewer wet days during these periods are likely to result in narrower rings. Indeed, Drew et al. (2014) observed that the short-term record-breaking rainfall associated with tropical cyclone Carlos in 2011 had little impact on growth increment of *C. intratropica* for that year, and our results in Table 2 show notionally stronger relationships with rain days (once a threshold is applied) than with rainfall amount. Drew et al. (2014) also suggested that narrow rings may usefully identify dry years. Our results that show higher moisture sensitivity of *C. intratropica* in SON and MAM (Figures 4, Appendix S2) with a DJF hiatus when moisture is unlikely to be limiting (Figures 4, Appendix S2), concur with this detailed monitoring work. Additionally, we note that the narrowest rings for both chronologies (1925 (MUR) and 1951 (KOR)) are associated with both low rainfall and a low number of rain days at one or both rainfall stations (Table S2). There also appears to be some correspondence between narrow rings (more than 1σ below mean ring width), and dry years (more than 1σ below the mean), or years that had relatively few (more than 1σ below the mean) rain days, for the first part of the 20th Century, but this pattern does not clearly persist for the latter part of the century (Table S2). This relationship with moisture conforms with the ecology of flora and fauna in this region that is intimately linked to the timing and pattern of rain (Woinarski et al., 2007).

Strong correlations with temperature (~July-October, MAM; Figure 4), evapotranspiration (MAM; Figure 4) and drought (Figure 4; Appendix S2) also concur with previous findings that temperature plays an important role in the moisture budget for the species (Drew et al. 2014). Stronger and more spatially consistent relationships between increment growth and the SPEI (and sc-PDSI; Figures 4; Appendix S2; Figures S5, S6) compared to precipitation (Figure 4, Appendix S2; Figure S3) could be associated with greater geographic variability in the incidence of precipitation and the presence of ground water.

The consistency of our statistical results with detailed physiological work supports selection of months at the start and end of the wet period of the year for hydroclimate reconstructions.

The potential of C. intratropica for hydrological reconstructions

Our analyses point to the importance of hydroclimate to ring widths in this species during the transition into (SON) and out of (MAM) the wettest months of the year in northern Australia. This in turn strongly points to the relevance of early/late starts and ends of the wet period of the year for incremental growth, in line with Drew et al. (2014). Based on our results, both total precipitation and streamflow in the region may be suitable targets for reconstruction at these times. Although not a variable commonly reconstructed, its potential link to the El Niño Southern Oscillation (ENSO; Smith et al., 2006; Cook and Heerdegen, 2001), means further investigation of the possibility for reconstructions of days of precipitation (> 5mm) over MAM would be worthwhile. We note that narrow rings in both chronologies often coincide with El Niño but not La Niña events (Table S2), although unfortunately, there is inadequate information to statistically test this.

Although interest is often focused on total precipitation received over the entire wet period, the significance of hydroclimate reconstructions for the transitional months should not be underestimated. These are key periods both for Indigenous peoples and ecological processes and are defined by particular activities, events, availability of foods and the presence of particular fauna (Table 3). Variability in the timing of monsoonal rain, especially at the start and end of the wet period (i.e. the duration of the wet period) will have critical impacts on land management and on ecological processes that in turn affect the availability of certain foods such as sugarbag honey or bush yams,

or breeding and migration cycles of some species (Redhead 1979; Vardon et al., 2001; Cook and Heerdegen 2001; Woinarski et al., 2007). Reconstructed climate variability at this time may therefore provide vital clues to some aspects of regional environmental history, providing baseline information about duration of the wet period prior to instrumental records. Daily information available from Australian Water Availability Project (Jones et al., 2009) data may help facilitate gridded reconstructions of duration of the wet period and this potential requires further investigation.

In general, the apparent correspondence between very narrow rings and dry conditions and our correlative results suggest that hydrological reconstructions from *C. intratropica* may be possible for either of the transitional periods here, (SON or MAM), but that care will need to be taken in selecting the target variable. While the potential of the species to reconstruct precipitation for either of these windows requires further investigation, results suggest that for drought – as defined by the SPEI or sc-PDSI – only reconstructions for MAM drought make sense (Figures 4, Appendix 2; Figures S5-S6). This is because the formulation of the drought indices used here is premised on the negative impact of increased temperature on moisture availability (see Vicente-Serrano et al., 2010 and references therein). This means that for a positive relationship with the SPEI to make sense, we would expect a positive relationship with precipitation and a simultaneously negative association with temperature. While MAM period meets this condition, JJA does not (Figure 4; Appendix S2; Figures S5-6). The association with evapotranspiration is also strongly negative for MAM, this being consistent with opposite relationships with temperature and precipitation at this time. Therefore, *C. intratropica* in this region appears ideally placed to reconstruct MAM drought. Nevertheless, the ability to reconstruct any hydrological variable needs to be properly considered in the context of a reconstruction model, and this is well beyond the scope of this paper.

A further important consideration will be the required sampling strategy. Based on the greater spatial coherence of correlations with the drought indices compared to precipitation shown in this study, drought index reconstruction is likely to require a lower site density than reconstructions of precipitation for which there is greater variability across the region. Importantly, neither of the sites presented in this study were sampled with dendroclimatology in mind and relatively weak relationships found with streamflow in particular, may reflect this.

Conclusions

In this paper we have presented two well-replicated and crossdated Australian *Callitris* tree-ring chronologies, and demonstrated the potential for dead *C. intratropica* trees that remain sufficiently intact over long periods of time to be included in chronologies. This demonstrates the potential to temporally and spatially extend the *C. intratropica* tree-ring network across northern Australia suitable for hydroclimate reconstructions over the past 250-300 years. An expanded network of well-replicated tree-ring chronologies for this region increases the potential for high-quality hydroclimate reconstructions in a region where there currently exist very few annually resolved multi-centennial palaeoclimate records. The KOR chronology extends the tree-ring based climate record back 86 years, and its response to climate is consistent with previous work.

For the first time, we demonstrate clear consistent and seasonal patterns in relationships between the chronologies and climate across the far north of Australia. This is an important basis for future hydroclimate reconstructions, although our results suggest that perhaps a broader region should be further tested. Overall, results indicate that reconstruction efforts should focus on hydroclimate variability for months that transition into and out of the wet period of the year. This strongly points to the

importance of the duration of the wet time of the year to wood formation in this species. Crucial ecological processes that support Indigenous land management and cultural practices occur during both these transitional periods and previous work has commented on the importance of duration of the wet period to regional flora and fauna. Given that variability in the length of the wet period may also be linked to ENSO, hydrological reconstructions from this species in this region may be particularly valuable for assessing past variability in this climate mode with an almost global reach.

References

Allen K. J., Cook, E.R., Francey, R.J., Michael, K. (2001) The climatic response of *Phyllocladus aspleniifolius* (Labill.) Hook. F. in Tasmania *Journal of Biogeography* 28: 305 - 316

Allen K.J., Ogden J., Buckley B.M., Cook E.R., Baker P.J. (2011) The potential to reconstruct broadscale climate indices associated with Australian droughts from Athrotaxis species, Tasmania. *Climate Dynamics* 37: 1799–1821

Allen, K.J., Fenwick P., Palmer, J.G., Nichols, S.C., Cook, E.R., Buckley, B.M., Baker P.J. (2017) A 1700-year *Athrotaxis selaginoides* tree-ring width chronology from southeastern Australia. *Dendrochronologia* 45: 90 - 100

Allen, K.J., Cook, E.R., Evans, R., Francey, R.J., Buckley, B.M., Palmer, J.G., Peterson, M.J., Baker, P.J. (2018) Lack of cool, not warm, extremes distinguishes late 20th Century climate in 979-year Tasmanian summer temperature reconstruction. *Environmental Research Letters* 13 034041

Baker, P.J., Palmer, J.G., D'Arrigo, R. (2008) The dendrochronology of *Callitris intratropica* in northern Australia: annual ring structure, chronology development and climate correlations. *Australian Journal of Botany* 56: 311–320

Becker, A., Finger, P., Meyer-Christoffer, A., Rudolf, B., Schamm, K., Schneider, U., Ziese, M. (2013) A description of the global land-surface precipitation data products of the Global Precipitation Climatology Centre with sample applications including centennial (trend) analysis from 1901-present. *Earth System Science Data* 5: 71–99

Bowman, D.M.J.S., Panton, W.J. (1993) Decline of *Callitris intratropica* R.T. Baker and H.G. Smith in the Northern Territory: implications for pre- and post-European colonization fire regimes. *Journal of Biogeography* 20: 373-381.

565 Bowman, D.M.J.S., MacDermott H.J., Nichols S.C., Murphy B.P. (2014) A grass−fire
566 cycle eliminates an obligate-seeding tree in a tropical savanna. *Ecology and Evolution*
567 4: 4185-4194.

568 Bowman, D.M.J.S., Haverkamp, C., Rann, K.D., Prior, L.D. (2018) Differential
569 demographic filtering by surface fires: how fuel type and fuel load affect sapling
570 mortality of an obligate seeder savanna tree. *Journal of Ecology* 106: 1010–1022.

571 Brodribb, T.J., Bowman, D.J.M.S., Nichols, S., Delzon, S., Burlett, R. (2010) Xylem
572 function and growth rate interact to determine recovery rates after exposure to extreme
573 water deficit. *New Phytologist* 188: 533-542

574 Brodribb, T.J., Bowman, D.M.J.S., Grierson, P.F., Murphy, B.P., Nichols, S., Prior,
575 L.D. (2013) Conservative water management in the widespread conifer genus Callitris.
576 *Aob Plants* 5: 1–11

577 Buckley B.M., Cook E.R., Peterson M.J., Barbetti, M. (1997) A changing temperature
578 response with elevation for *Lagarostrobos franklinii* in Tasmania, Australia, *Climatic*
579 *Change* 36: 477-498

580 Bunn, A.G. (2010) Statistical and visual crossdating in R using the dplR library.
581 *Dendrochronologia* 28: 251-258

582 Cook, B.I., Palmer, J.G., Cook, E.R., Turney, C.S.M., Allen, K., Fenwick, P.,
583 O'Donnell, A., Lough, J.M., Grierson, P.F., Ho, M., Baker, P.J. (2016) The paleoclimate
584 context and future trajectory of extreme summer hydroclimate in eastern Australia.
585 *Journal of geophysical Research: Atmospheres* 121: 12,280–12,838

586 Cook, E.R., Buckley, B.M., D'Arrigo, R.D., Peterson, M.J. (2000) Warm-season
587 temperatures since 1600BC reconstructed from Tasmanian tree rings and their
588 relationship to large-scale sea surface temperature anomalies. *Climate Dynamics*
589 16:79-91

590 Cook, E.R., Seager, R., Cane, M.A., Stahle, D.W. (2007) North American drought:
591 reconstructions, causes, and consequences. *Earth-Science Reviews* 81: 93–134

592 Cook, E.R., Anchukaitis, K.J., Buckley, B.M., D'Arrigo, R.D., Jacoby, G.C., Wright,
593 W.E. (2010) Asian monsoon failure and megadrought during the last millennium.
594 *Science* 328: 486-489

595 Cook, E.R. et al. (2015) Old World megadroughts and pluvials during the Common Era.
596 *Scientific Advances* e1500561, 1-9

597 Cook, G.D. and Heerdegen, R.G. (2001) Spatial variation in the duration of the rainy
598 season in monsoonal Australia. *International Journal of Climatology* 21: 1723-1732

599 Cullen, L. and Grierson P. (2007) A stable oxygen, but not carbon, isotope chronology
600 of *Callitris columellaris* reflects recent climate change in north-western Australia.
601 *Climatic Change* 85: 213-229

602 Cullen, L. and Grierson P. (2009) Multi-decadal scale variability in autumn-winter
603 rainfall in south-western Australia since 1655 AD as reconstructed from *Callitris*
604 *columellaris*. *Climate Dynamics* 33: 433-444

605 D'Arrigo, R.D., Baker, P., Palmer, J., Anchukaitis, K., Cook, G. (2008) Experimental
606 reconstruction of monsoon drought variability for Australasia using tree rings and
607 corals. *Geophysical Research Letters* 35, L12709, doi: 10.1029/2008GL034393

608 Drew, D.M., Richards, A.E., Downes, G.M., Cook, G.D., Baker, P. (2011) The
609 development of seasonal tree water deficit in *Callitris intratropica*. *Tree Physiology* 00:
610 1 – 12, doi: 10.1093/treephys/tpr031

611 Drew, D.M., Richards, A.E., Cook, G.D., Downes, G.M., Gill, W., Baker, P.J. (2014)
612 The number of days on which increment occurs is the primary determinant of annual
613 ring width in *Callitris intratropica*. *Trees* 28: 31 - 40

614 Farjon, A. (2010) *A Handbook of the World's Conifers*. *Vol I*. Koninklijke Brill NV,
615 Leiden, The Netherlands, 526pp.

616 Feng, X., Porporato, A., & Rodriguez-Iturbe, I. (2013). Changes in rainfall seasonality
617 in the tropics. *Nature Climate Change* 3, 811–815

618 Fritts, H.C., 1976, *Tree Rings and Climate* Academic Press New York. 567pp.

619 Fu, G., Charles, S.P., Timbal, B., Jovanovic, B., Ouyang, F. (2015) Comparison of
620 NCEP-NCAR and ERA-Interim over Australia. *International Journal of Climatology*
621 36: 2345-2367

622 Guttman, N.B. (1998) Comparing the palmer Drought Severity Index and the
623 Standardized precipitation Index. *Journal of the American Water Resource Association*
624 34: 113-121

625 Hanna, D.P., Falk, D.A., Swetnam, T.W., Romme, W. (2018) Age-related climate
626 sensitivity in *Pinus edulis* at Dinosaur national Monument, Colorado, USA.
627 *Dendrochronologia* 52: 40-47

628 Haines, H.A., Olley, J.M., English, N.B., Hua, Q. (2018) Anomalous ring identification
629 in two Australian subtropical Araucariaceae species permits annual ring dating and
630 growth-climate relationship development. *Dendrochronologia* 49: 16-28

631 Haines, H.A., Gadd, P.S., Palmer, J., Olley, J.M., Hua, Q., Heijnis, H. (2018) A new
632 method for dating tree-rings in trees with faint, indeterminate ring boundaries using the
633 Itrax core scanner. *Palaeogeography, Palaeoclimatology, Palaeoecology* 497: 234-243

634 Hammer, G.L. (1981) Site classification and tree diameter-height-age relationships for
635 cypress pine in the Top End of the Northern Territory. *Australian Forestry* 44: 35–41

636 Hammer, G.L. (1983) *Growth of cypress pine (Callitris columellaris F.Muell) in the*
637 *Northern Territory - a modelling approach*. Unpub. Master of Forest Science Thesis,
638 University of Melbourne.

639 Harris, I., Jones, P.D., Osborn, T.J. and Lister, D.H. (2014) Updated high-resolution
640 grids of monthly climatic observations – the CRU TS3.10 Dataset. *International*
641 *Journal of Climatology* 34: 623–642

642 Heinrich I., Weidner K., Helle G., Vos H., Banks J.G.C. (2008) Hydroclimatic variation
643 in far north Queensland since 1860 inferred from tree rings. *Palaeogeography,*
644 *Palaeoclimatology, Palaeoecology* 270: 116-127

645 Heinrich I., Weidner K., Helle G., Vos H., Lindesay J., Banks J.C.G. (2009)
646 Interdecadal modulation of the relationship between ENSO, IPO and precipitation:
647 insights from tree rings in Australia. *Climate Dynamics* 33:63–73

648 Holmes, R (1983) Computer-assisted quality control in tree-ring dating and
649 measurement. *Tree-Ring Bulletin* 43:69-75

650 Jeong, D.I., Sushama, L., Khaliq, M.N. (2014) The role of temperature in drought
651 projections over North America. *Climatic Change* 127:289–303

652 Jones, D., Wang, W. and Fawcet, R. (2009) High-quality spatial climate data sets for
653 Australia. *Australian Meteorological and Oceanographic Journal* 58: 233-248

654 Kahle, D. and Wickham, H. (2013) ggmap: Spatial Visualization with ggplot2. The R
655 Journal, 5(1), 144-161

656 Lawes, M.J., Taplin, P., Bellairs, S.M., Franklin, D.C. (2013) A trade-off in stand size
657 effects in the reproductive biology of a declining tropical conifer *Callitris intratropica*.
658 *Plant Ecology* 214: 169 – 174

659 Lunt, I.D., Zimmer, H.C., Cheal, D.C. (2011) The tortoise and the hare? Post-fire
660 regeneration in mixed *Eucalyptus – Callitris* forest. *Australian Journal of Botany* 59:
661 575-581

662 Melvin, T.M. and Briffa, K.R. (2008) A "signal-free" approach to dendroclimatic
663 standardisation. *Dendrochronologia* 26: 71–86

664 O'Donnell, A.J., Cullen, L.E., McCaw, L., Boer, M.M., Grierson, P.F. (2010)
665 Dendroecological potential of *Callitris preisii* for dating historical fires in semi-arid
666 shrublands of southern Western Australia. *Dendrochronologia* 28: 37-48

667 O'Donnell, A.J., Cook, E.R., Palmer, J.G., Turney, C.S.M., Page, G.F.M., Grierson,
668 P.F. (2015) Tree rings show recent high summer-autumn precipitation in northwest
669 Australia is unprecedented within the last two centuries. *PLOSone* 10: e0128533

670 O'Donnell, A.J., Cook, E.R., Palmer, J.G., Turney, C.S.M., Grierson, P.F. (2018)
671 Potential for tree rings to reveal spatial patterns of past drought variability across
672 western Australia. *Environmental Research Letters* 13, 024020

673 Ogden, J. (1981) Dendrochronological studies and the determination of tree ages in the
674 Australian tropics. *Journal of Biogeography* 8: 405-420

675 Palmer, W.C. (1965) *Meteorological drought*. Office of Climatology Research paper
676 45, Weather Bureau Washington DC, 58 pp.

677 Palmer, J.G., Cook, E.R., Turney, C.S.M., Allen, K., Fenwick, P., Cook, B.I.,
678 O'Donnell, A., Lough, J., Grierson, P., Baker, P. (2015) Drought variability in the
679 eastern Australia and New Zealand summer drought atlas (ANZDA, CE 1500 – 2012)
680 modulated by the Interdecadal Pacific Oscillation. *Environmental Research Letters* 10,
681 124002

682 Pearson, S.G. and Searson, M.J. (2002) High-resolution data from Australian trees.
683 *Australian Journal of Botany* 50: 431-439

684 Pearson, S., Hua, Q., Allen, K., Bowman, D.M.J.S. (2011) Validating putatively cross-
685 dated *Callitris* tree-ring chronologies using bomb-pulse radiocarbon analysis.

686 *Australian Journal of Botany* 59: 7–17

687 Piggins, J. and Bruhl, J.J. (2010) Phylogeny reconstruction of *Callitris* Vent.
688 (Cupressaceae) and its allies leads to inclusion of *Actinostrobus* within *Callitris*
689 *Australian Systematic Botany* 23: 69-93

690 Prior, L. D., Bowman, D. M. J. S., Eamus, D. (2004a) Seasonal differences in leaf
691 attributes in Australian tropical tree species: family and habitat comparisons.
692 *Functional Ecology*18: 707–718

693 Prior, L.D., Eamus, D., Bowman, D.M.J.S. (2004b) Tree growth rates in north
694 Australian savanna habitats: seasonal patterns and correlations with leaf attributes.
695 *Australian Journal of Botany* 52, 303-314

696 Prior, L.D., Lee, Z., Brock, C., Williamson G.J., Bowman, D.M.J.S. (2010) What limits
697 the distribution and abundance of the native conifer *Callitris glaucophylla* in the West
698 MacDonnell Ranges central Australia? *Australian Journal of Botany* 58: 554-564

699 Prior L.D., McCaw, W.L., Grierson, P.F., Murphy, B.P., Bowman, D.M.J.S. (2011)
700 Population structures of the widespread Australian conifer *Callitris columellaris* are a
701 bio-indicator of continental environmental change. *Forest Ecology and Management*
702 262, 252-262

703 Radford, I.J., Andersen, A.N., Graham, G., Trauernicht, C. (2013) The fire refuge value
704 of patches of a fire-sensitive tree in fire-prone savannas: *Callitris intratropica* in
705 northern Australia. *Biotropica* 45: 594-601

706 Redhead, T.D. (1979) On the demography of *Rattus sordidus colletti* in monsoonal
707 Australia. *Australian Journal of Ecology* 4: 115-136

708 Russell-Smith, J. (2006) Recruitment dynamics of the long-lived obligate seeders
709 *Callitris intratropica* (Cupressaceae) and *Petraeomyrtus punicea* (Myrtaceae).
710 *Australian Journal of Botany* 54: 479-485

711 Sakaguchi S, Bowman D, Prior L, Crisp M, Linde C, Tsumura Y, Isagi Y (2013)
712 Climate, not Aboriginal landscape burning, controlled the historical demography and
713 distribution of fire-sensitive conifer populations across Australia. *Proceedings of the*
714 *Royal Society B: Biological Sciences* 280, 20132182.

715 Santini, N.S., Hua, Q., Schmitz, N., Lovelock, C.E. (2013) Radiocarbon dating and
716 wood density chronologies of mangrove trees in arid western Australia. *PLOSone* 8:
717 e80116

718 Schneider, U., Becker, A., Finger, P., Meyer-Christoffer, A., Ziese, M., Rudolf, B.
719 (2014) GPCC's new land surface precipitation climatology based on quality-controlled
720 in situ data and its role in quantifying the global water cycle. *Theoretical and Applied*
721 *Climatology* 115: 15-40

722 Smith, I.N., Wilson, L., Suppiah, R. (2006) Characteristics of the northern Australian
723 rainy season. *Journal of Climate* 21: 4298-4311

724 Stahle, D.W., Cook, E.R., Burnette, D.J., Villanueva, J., Cerano, J., Burns, J.N., Griffin,
725 D., Cook, B.I., Acuna, R., Torbenson, M.C.A., Sjezner, P., Howard, I.M. (2016) the
726 Mexican Drought Atlas: tree-ring reconstructions of the soil moisture balance during
727 the late pre-Hispanic, colonial, and modern eras. *Quaternary Science Reviews* 149: 34–
728 60

729 Stokes, M.A. and Smiley, T.L. (1968) *Introduction to Tree-ring Dating.* University of
730 Chicago Press, Chicago

731 Trauernicht, C., Murphy, B.P., Portner, T.E., Bowman, D.M.J.S. (2012) Tree cover-fire
732 interactions promote the persistence of a fire-sensitive conifer in a highly flammable
733 savanna. *Journal of Ecology* 100: 958-968

734 Vardon, M.J., Brocklehurst, P.S., Woinarski, J.C.Z., Cunningham R.B., Donnelly C.F.,
735 Tiderman, C.R. (2001) Seasonal habitat use of flying-foxes, *Pteropus alecto* and *P.*
736 *scapilatus* (Megachiroptera), in monsoonal Australia. *Journal of Zoological Society of*
737 *London* 253: 523-535

738 Verdon-Kidd, D.C., Hancock, G.R., Lowry, J.B. (2017) A 507-year rainfall and runoff
739 reconstruction for the Monsoonal north west, Australia derived from remote
740 paleoclimate archives. *Global and Planetary Change* 158: 21-35

741 Vicente-Serrano, S.M., Beguería, S., López-Moreno, J.I. (2010) A Multi-scalar drought
742 index sensitive to global warming: The Standardized Precipitation Evapotranspiration
743 Index – SPEI. *Journal of Climate* 23: 1696-1718
744 Vicente-Serrano, S.M., Beguería, S., López-Moreno, J.I., Angulo, M., El Kenawy, A.
745 (2010) A global 0.5° gridded dataset (1901-2006) of a multiscalar drought index
746 considering the joint effects of precipitation and temperature. *Journal of*
747 *Hydrometeorology* 11: 1033-1043

748 Wells, N., Goddard, S., Hayes, M.J. (2004) A self-calibrating Palmer Drought Severity
749 Index. *Journal of Climate* 15: 2335-2351

750 Wigley TML, Briffa KR, Jones PD (1984) On the average value of correlated time
751 series, with applications in dendroclimatology and hydrometeorology. *Journal of*
752 *Climate and Applied Meteorology* **23**: 201 – 213

753 Witt, G.B., English, N.B., Balanzategui, D., Hua, Q., Gadd, P., Heijins, H., Bird, M.
754 (2017) The climate reconstruction potential of *Acacia cambagei* (gidgee) for semi-arid

regions of Australia using stable isotopes and elemental abundances. *Journal of Arid Environments* 136: 19-27

Woinarski, J.C.Z., Hempel, C., Cowie, I., Brenna, K., Kerrigan, R., Leach, G., Russell-Smith, J. (2006) Distributional pattern of plant species endemic to the Northern Territory, Australia. *Australian Journal of Botany* 54: 627-640

Woinarski, J., Mackey, B., Nix, H., Traill, B. (2007) *The Nature of Northern Australia* ANU E-Press, Canberra Australia, 125pp.

Yates, C. and Russell-Smith, J. (2003) Fire regimes and vegetation sensitivity analysis: an example from Bradshaw Station, monsoonal northern Australia. *International Journal of Wildland Fire* 12: 349-358

Figures and Tables in Supplementary Appendices

Figure S1. Skeleton plots for the two sites

Figure S2. Correlation of all tree-ring series at a site to master series for each chronology

Figure S3. Boxplots of regional monthly correlations of chronologies with climate variables

Figure S4. Correlations between chronologies and site temperature and precipitation

Figure S5. Boxplots of Pearson correlations of KOR and MUR with variously scaled SPEI indices

Figure S6. As for Figure S3, but for PDSI

Figure S7. Regional correlations, chronologies with drought indices (1903 – 1973)

Figure S8. Regional correlations, chronologies with drought indices (1903-1973 MUR; 1903-2015 KOR)

Table S1. Narrow rings in chronologies, years total precipitation total and days low, El Nino events

Table S2. Average intercorrelations amongst all gridded climate data for climate variables

Figure captions

Figure 1: Top: Map showing location of Top End and area for which climate correlations calculated. Bottom: tree-ring site locations, location of East Alligator River streamflow gauge, and location of the four high quality precipitation stations used to show trends over the 20th Century. Temperature data series also from the Darwin meteorological station. The white square denoting the Litchfield National Park shows the existence of two other small collections of *C. intratropica* (for details, see Pearson et al., 2011). The ggmap package in R was used to produce the map showing sites (Kahle and Wickham 2013).

Figure 2: Average monthly temperature and precipitation for the study region, averaged from the CRU temperature data and GPCC precipitation for the identified region (Figure 1). Blue bars are precipitation, solid black line is maximum temperature and dashed line is minimum temperature. B. Average annual temperature at Darwin (August-September year; station 014015) shown as z-scores. Solid line is maximum temperature and dashed line minimum temperature; C. Time series of precipitation z-scores for two of four high quality precipitation stations in region shown in Figure 1 (Darwin airport 014015 solid line; Warruwi 014042 dotted line); D Time series of precipitation z-scores for two of four high quality precipitation stations in region shown in Figure 1 (Oenpelli 014042 solid line, Katherine 014902 dotted line). Note the differing scales on the x-axes for temperature and precipitation series. Meteorological data for these stations was obtained from the Bureau of Meteorology (www.bom.gov.au).

Figure 3: A. The two chronologies and sample depths. B. Running EPS and RBar for the two sites, calculated for successive 50-year windows. C. Spectra of the two sites. Statistically significant ($p < 0.05$) periodicities include 64.1, 4.57, 2.91 years (KOR)

and 64.1 and 4.74 years (MUR). The dotted line represents the 95% significance level and the dashed line, the 99% significance level.

Figure 4: Boxplots of correlations between the two chronologies and gridded climate data averaged over 3-monthly periods for the period 1902 – 2015 (KOR temperature and drought indices), 1901-2015 (KOR; precipitation) and 1902 – 1973 (MUR; temperature and drought indices) and 1901 – 1973 (MUR; precipitation). The SPEI plots are for the SPEI-3, for the same months as the other climate variables. A - B mean temperature (107 grid cells); C-D maximum temperature (107 grid cells); E-F minimum temperature (2017 grid cells); G-H precipitation (118 grid cells); I-J potential evapotranspiration (107 grid cells), K-L SPEI-3 (107 grid cells). The left column shows correlations for KOR and the right, for MUR. The box represents the intrequartile range and the whiskers for each box extend out to the maximum and minimum values. Coloured boxes are shown for those periods in which correlations for all grid cells are positive (negative) while grey boxes are used for periods in which there are both positive and negative values. Dashed lines represent the 95% significance limits. A 'p' in front of the x-axis label denotes the year prior to growth.

Figure 5. KOR chronology plotted against streamflow at East Alligator River gauge for (A) Aug-Jul, (B) Sep-Nov, (C) Dec-Feb and (D) Mar-May. Black line is KOR chronology, red line with points is streamflow. Note the visually strong relationships with MAM streamflow over the past ~15 years.

Tables

Statistic	KOR	MUR	PC	HS
Chronology period	1761 - 2015	1845 - 1973	1847 - 2006	1964 - 2004
n (N^{+})	165 (129)	69 (43)	30 (14)	64 (20)
Average EPS	0.92	0.95	0.94	-
Period for which EPS > 0.85	1803-2015	1846-1973	1857-2006‡	-
Average RBar	0.35	0.42	0.67	-
Median segment length	86 (43,188)	74 (39,127)	96 (56,160)	40
Average autocorrelation	0.585	0.556	0.56	-
MS	0.4	0.4	0.35	0.26
MISC	0.55	0.46	0.74	0.69

Table 1: Chronology statistics for the KOR and MUR chronologies presented here as well as the previously published Pine Creek (PS) and Howard Springs (HS) sites (Baker et al., 2008) where data/information available. n (N) is the number of samples (trees) making up the chronology. $^{+}$Note that N is an estimate. Due to labelling of samples – particularly for old MUR samples - it was not always possible to identify whether two separate cores came from a single tree. ‡ indicates that this is not provided in the original paper, but has been recalculated here using the signal-free version of the chronology (see methods). This will result in small differences with the original chronology. Median segment length refers to the median length of an individual sample in the

839 chronology. Figures in brackets are the minimum and maximum lengths respectively.
840 Average RBar and EPS are calculated for the entire chronologies; for year –to-year
841 variation, see Figure 4B. Average autocorrelation reports the average lag 1
842 autocorrelation. Figures shown in the table for PC relate to the samples used in the
843 final chronology rather than all samples collected (as shown in Baker et al. 2008).

844

	Oenpelli		Warruwi		
Amount of precipitation					
	KOR (1910-2013)	MUR (1910-1973)	KOR (1916-2015)	MUR (1916-1973)	Average
Aug– Jul	***0.31***	0.22	***0.38***	***0.33***	0.31
Dec-Feb	-0.07	0.00	0.03	0.12	0.08
Sept – Nov	***0.30***	*0.27*	***0.37***	0.21	0.29
Mar- May	***0.43***	*0.27*	***0.42***	***0.35***	0.37
Number of days of precipitation					
Aug– Jul	*0.25* (***0.53***)	***0.39 (0.41)***	0.18 (***0.44***)	0.24 (***0.40***)	0.27 (0.45)
Dec-Feb	0.15 (*0.23*)	0.21 (0.21)	0. 06 (0.16)	0.03 (0.18)	0.11 (0.20)
Sep – Nov	0.14 ***(0.39***)	*0.25* (0.24)	0.00 (*0.27*)	0.05 (0.22)	0.11 (0.28)
Mar - May	***0.41*** (***0.63***)	***0.48 (0.49)***	0.17 (***0.52***)	0.17 (***0.51***)	0.31 (0.54)

845 **Table 2:** Correlations between the two chronologies and rainfall at the two nearest high
846 quality rainfall stations. Periods available for each analysis are noted next to the site
847 names). Figures in brackets for number of rain days are correlations for days when rain
848 exceeded 5mm. Correlations with both the amount of precipitation and the number of
849 days of rain are nominally highest for March-May, and correlations with the number of
850 days of rain are generally nominally higher than those with the absolute amount of rain
851 in each case. Italicised correlations for individual sites are significant at 0.05 level and
852 bold italics indicate significance at the 0.01 level.
853
854
855
856

Window	**Indigenous calendar**	**Season name/part**	**Characteristics**	Impt foods/othrs…from Indigenous calendars
JJA	Maung	Wumulukuk (March-July)	SE trade winds (Jun-Jul)	'Knock'em down winds', tamarind, wattle and eucalypt flowers, sugarbag harvesting,, grass and trees dry out, time to burn off
	Tiwi	Kumunupari (Mar-Aug)	Dry, fire and smoke	Plants and animals: yams, water lily, bush pumpkin, long yam, mud mussel, bush turkey, carpet python, turtles
	Jawoyn	Malaparr (Jun-Aug)	Cooler	
SON	Maung	Walmatpalmat (Nov-Feb), Kinyjapurr (Sep-Oct)	Heavy rain (Nov) Hot and humid, strong SE winds (Aug) SE and NW winds (Sep-Oct)	Kinyjapurr: rougher seas, thicker clouds, storms begin, wild apple, billy goat plums, bush potato sprouting Walmatpalmat : Bushfires, cyclones, new plant shoots, tamarind flowers, mangoes, wild

				apple, green plums, yam shoots, crab moulting
	Tiwi	Tiyari	Hot weather, high humidity	Plants and animals: cycad, peanut tree, magpie geese, dugong, whistling duck, mangrove worms
	Jawoyn	Worrwopmi (Sep-Oct) Wakaringding (Nov-Dec)	Monsoonal buildup (Sep-Dec), first rains (Nov-Dec)	
DJF	Maung	Walmatpalmat	Heavy rain	Bushfires, cyclones, new plant shoots, tamarind flowers, mangoes, wild apple, green plums, yam shoots, crab moulting
	Tiwi	Jamutakari	Wet season, consistent rain, NW winds, storms	Plants and animals: Green plums, pink bush apple, bush potato, northern brush tail possum, saltwater crocodile, barramundi, crested tern eggs, cocky apple

	Jawoyn	Wakaringding (Nov-Dec), Jiorrk (Jan-Feb)	First rains (Nov-Dec) Main part of wet season 9Jan-Feb)	
MAM	Maung	Wumulukuk (March-July)	Cold weather NW-SE winds (Mar-Apr; ‘knock-‘em down winds)	Tamarind, wattle and eucalypt flowers, sugarbag harvesting,, grass and trees dry out, time to burn off
	Tiwi	Kumunupari (Mar-Aug)	Dry, fire and smoke	Plants and animals: yams, water lily, bush pumpkin, long yam, mud mussel, bush turkey, carpet python, turtles
	Jawoyn	Bungarung (Mar-Apr) Jungalk (Apr-May)	Last of the rains, drying Hot/dry	

857

858 **Table 3**: Monthly windows used in the text and their correspondence to three local
859 Indigenous weather calendars for northern Australia available at :
860 http://www.bom.gov.au/iwk/ . Information summarised from the website. Note that
861 there is not a perfect correspondence to the windows used in this study. For minor
862 seasons and additional details regarding flora and fauna of importance during these
863 seasons, see the website above.
864

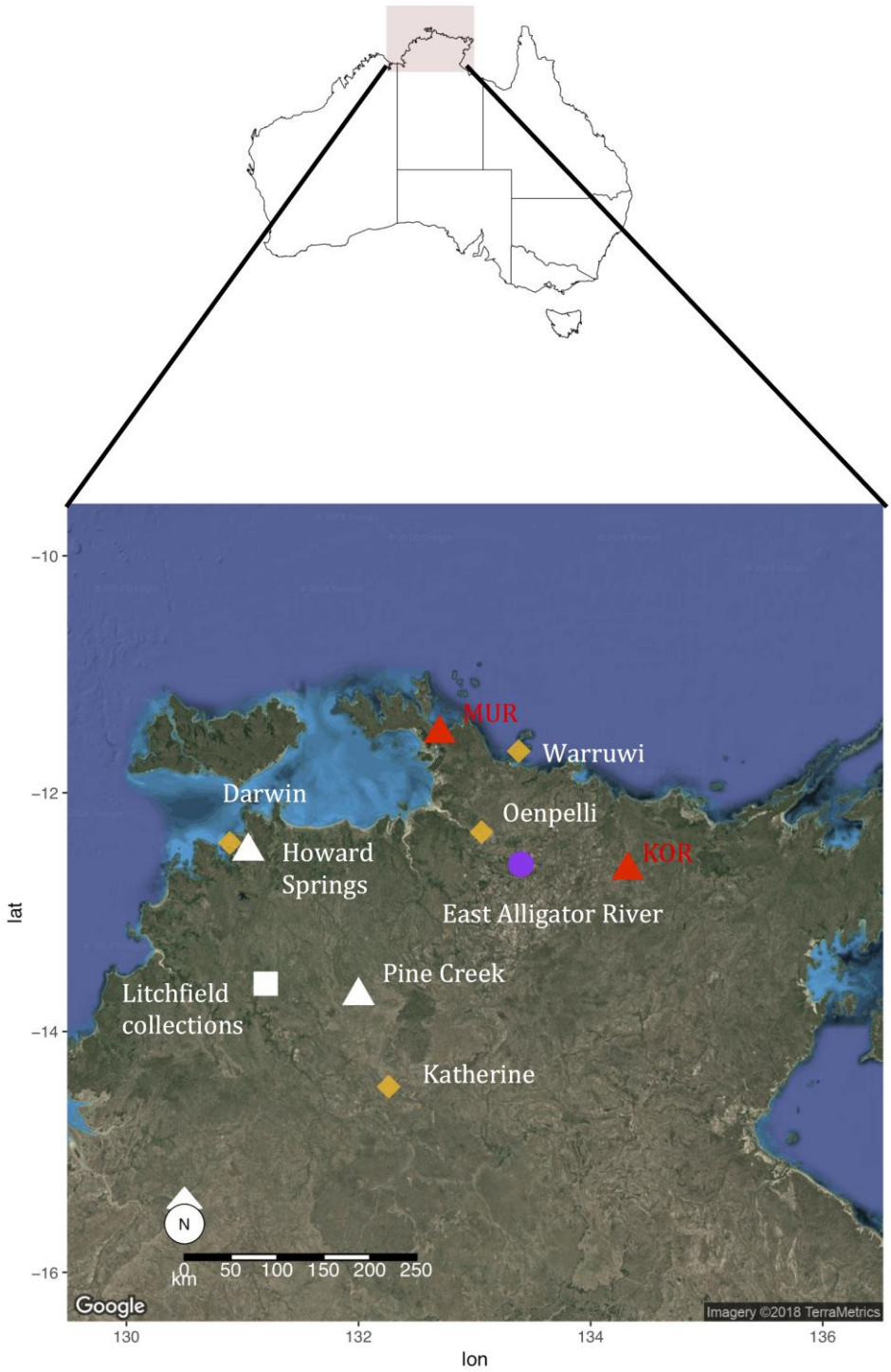

865
866
867 Fig. 1